# Dynamic recrystallization mechanisms operating in a Ni–20%Cr alloy under hot-to-warm working

N. Dudova [a,*], A. Belyakov [a], T. Sakai [b], R. Kaibyshev [a]

[a] *Belgorod State University, Belgorod 308015, Russia*
[b] *UEC Tokyo (The University of Electro-Communications), Chofu, Tokyo 182-8585, Japan*

**Abstract**

The structural mechanisms responsible for the development of new grains in a Ni–20%Cr alloy during hot-to-warm working were studied in compression at temperatures of 500–950 °C. A bilinear relationship between the flow stresses and the dynamic grain sizes was obtained with an inflection point at $7 \times 10^{-3}$ $G$. The dynamic grain size can be related to the flow stress through power-law functions with grain size exponents of −0.7 and −0.25 for low and high flow stresses, respectively. The variation of the stress versus grain size dependence is attributed to the change in mechanisms of new grain development from discontinuous to continuous reactions with increasing flow stress. The former is associated with the grain boundary bulging and the latter is related to a strain-induced phenomenon involving the development of large angular misorientations between deformation subgrains after large strains.

## 1. Introduction

Plastic working accompanied by dynamic recrystallization (DRX) is one of most promising methods for the formation of micron-, submicron- and nano-scale structures in a variety of metals and alloys [1–4]. Controlling the microstructure through DRX requires detailed information about the relationship between deformation conditions and resulting grain size. The main features of DRX in metallic materials have been reasonably well ascertained for hot working conditions, which lead to the formation of micron-scale grains. The development of DRX is associated with the formation of new grains, the size of which ($D$) can be expressed by a power-law function of temperature-compensated strain rate or flow stress ($\sigma$) as follows:

$$\sigma/G = AD^n, \tag{1}$$

where $A$ is a constant, $G$ is the shear modulus and $n$ is the grain size exponent, which is about −0.7 for hot working conditions [2–4].

The two main types of DRX operating in metallic materials are distinguished by the nature of their deformation behaviour and microstructure evolution under hot working [4–21]. Discontinuous DRX (DDRX) is associated with a bulging mechanism operating in materials with relatively low stacking fault energies [2,4,11,13,20]. The local migration, i.e. bulging, of grain boundaries leads to the formation of nuclei, which then grow out and consume a deformed matrix resulting in increased dislocation density, and providing strain softening. The large DRX grains are deformed upon further straining and taken up by new DRX nuclei. This leads to a dynamically constant average grain size. Since the DRX microstructure that evolves during processing actually consists of two structural components, i.e. dynamic grains in various hardened stages and new recrystallized grains, this process is considered to be a discontinuous phenomenon [2–4,15]. The structural changes in metallic materials with high stacking fault

energies are sometimes referred to as continuous DRX (CDRX) [5,7–10,12,14–19]. This process includes the formation of stable three-dimensional arrays of deformation low-angle boundaries (LABs) followed by their gradual transformation into high-angle grain boundaries (HABs) upon straining, which finally results in the development of recrystallized grains.

On the other hand, limited data is available on the nature of DRX under warm working conditions despite the fact that the formation of ultrafine grains after sufficiently large strains offers a feasible route to process metallic materials into submicrocrystalline or nanocrystalline states by a simple deformation method [15,19,22–28]. In those cases, the new grains result from a kind of strain-induced continuous reaction, including the formation of deformation-induced LABs and a gradual increase in their misorientations up to large angles, which is inherent in regular grain boundaries. Under warm working conditions, the grain size exponent in the power-law relationship between flow stress and DRX grain size was shown to be about half of that observed in hot working [15,22,25,27]. With increasing flow stress, therefore, the size of new grains rapidly decreases and becomes almost the same as the size of preceding deformation subgrains. The subgrain size can also be expressed by Eq. (1) but using an exponent of approximately 1 [1,4,8,25,27,29]. In the range of high flow stresses, however, there is still ambiguity about the relationship between the flow stresses and the sizes of structural elements.

The main aim of the present work is to examine the structural mechanisms leading to new grain evolution under hot-to-warm working. Specific attention was paid to the variation of DRX mechanisms with temperature. The second aim is to consider how DRX mechanisms affect the recrystallization behaviour for a range of warm working. A Ni–20%Cr alloy was used as a typical dilute alloy with low stacking fault energy.

## 2. Materials and methods

Ni–20%Cr alloy (21Cr–1.1Si–0.3Mn–0.75Fe–0.31Al–0.08Ti–0.35Cu–0.05C and balance Ni, all in wt.%) with an initial grain size of 80 μm was examined. Cylindrical samples 12 mm in length and 10 mm in diameter were compressed at temperatures ranging from 500 to 950 °C under an initial strain rate of $7 \times 10^{-4}\,s^{-1}$ followed by quenching with a water jet immediately after the deformation was stopped. The structural investigations were carried out on the specimen sections parallel to the compression axis by using an Olympus GX70 microscope, a Quanta 600FEG scanning electron microscope equipped with an electron back-scattering diffraction pattern (EBSP) analyser incorporating an orientation imaging microscopy (OIM) system, and a JEM-2100 transmission electron microscope. The OIM images were subjected to a cleanup procedure, setting a minimal confidence index of 0.05. Detailed analysis of crystallographic orientations among fine (sub)structural elements was carried out by the TEM Kikuchi-line technique. The grain/subgrain size was measured on the TEM micrographs by a linear intercept method, counting all clearly defined grain/subgrain boundaries. The dislocation density was measured by counting the individual dislocations in grain/subgrain interiors on at least four arbitrary selected typical TEM images for each data point.

## 3. Results

### 3.1. Stress–strain behaviour

A series of stress–strain ($\sigma$–$\varepsilon$) curves for the Ni–20%Cr alloy is shown in Fig. 1. Two distinctly different temperature intervals can be distinguished from the shape of these $\sigma$–$\varepsilon$ curves. At $T > 700$ °C, which corresponds to relatively low flow stresses below 500 MPa, the plastic flow attains steady state following a peak stress at relatively low strains of ~0.3. On the other hand, extensive strain hardening takes place at $T \leqslant 700$ °C. The rate of strain hardening gradually decreases down to a negligibly small value with strain. No strain softening is observed at $T < 700$ °C in the range of strains examined when the flow stresses are above 500 MPa. Decreasing the temperature leads to an increase in strain, where the strain hardening approaches its minimal value. At 500 °C, the deformation behaviour is characterized by the extensive hardening within the strain range studied.

### 3.2. Deformation microstructures

Typical deformation microstructures evolved at strain of $\varepsilon = 0.7$ at various temperatures are shown in Fig. 2. At 900 °C, DRX results in significant grain refinement (Fig. 2a). The fraction of new recrystallized grains amounts to ~0.6; their average size is ~3 μm. Some unrecrystallized, and hence work-hardened, coarse grains, which are portions of original grains, are highly elongated crosswise to

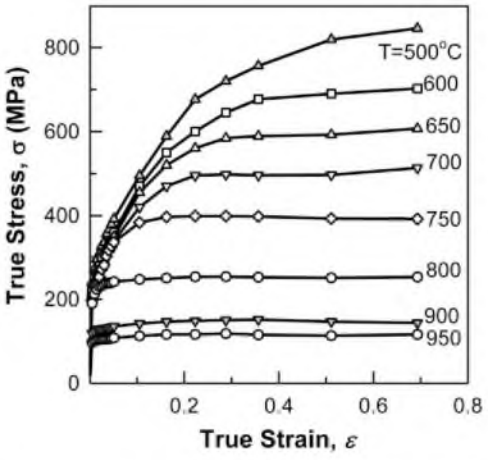


Fig. 1. True stress–true strain curves for Ni–20%Cr alloy strained by compression at different temperatures.

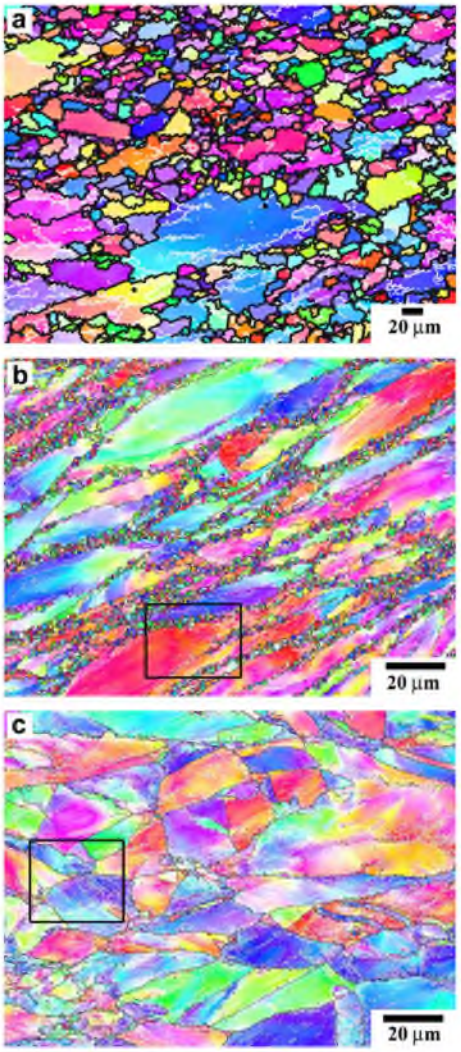


Fig. 2. Typical OIM pictures of Ni–20%Cr alloy strained to 0.7 at: (a) 900 °C; (b) 700 °C; and (c) 500 °C. White and black lines correspond to subgrain/grain boundaries with misorientations of $2° \leqslant \theta < 15°$ and $15° \leqslant \theta$, respectively.

the compression axis. At 700 °C, the deformation structure is characterized by pancake-shaped original grains that are decorated with chains of ultrafine grains (Fig. 2b). The formation of new grains takes place along the original grain boundaries, resulting in the development of the so-called necklace microstructure [2,8,13,15]. The decrease in deformation temperature leads to a reduction in both the volume fraction of new grains and their size to ~0.32 and ~0.6 μm, respectively.

At 500 °C, the deformation microstructure looks like a typical cold-worked one (Fig. 2c). A number of deformation-induced LABs is involved within original grains, which are elongated towards the direction of metal flow. In contrast to conventional cold-worked microstructures [8], however, the boundaries of original grains in Fig. 2c are frequently serrated and a few submicrometer-scale grains are observed near initial grain boundaries, especially at triple junctions. It can be concluded that plastic working of Ni–20%Cr alloy at temperatures of 500–950 °C results in the development of new grains, i.e. DRX, the features of which depend on processing conditions. Let us consider the structural mechanisms responsible for new grain evolution during deformation first at temperatures of 900 and 500 °C, which are clearly differentiated by the stress–strain behaviours and the grain structures developed, and then at 700 °C, where transient behaviour is observed, in more detail.

### 3.3. DRX at 900 °C

Fig. 3 shows a typical OIM image of microstructure evolved at $\varepsilon = 0.36$, which corresponds to the peak stress on the flow curve (Fig. 1). It can clearly be seen that the new fine grains develop at original boundaries and at triple junctions. The development of new grains due to grain

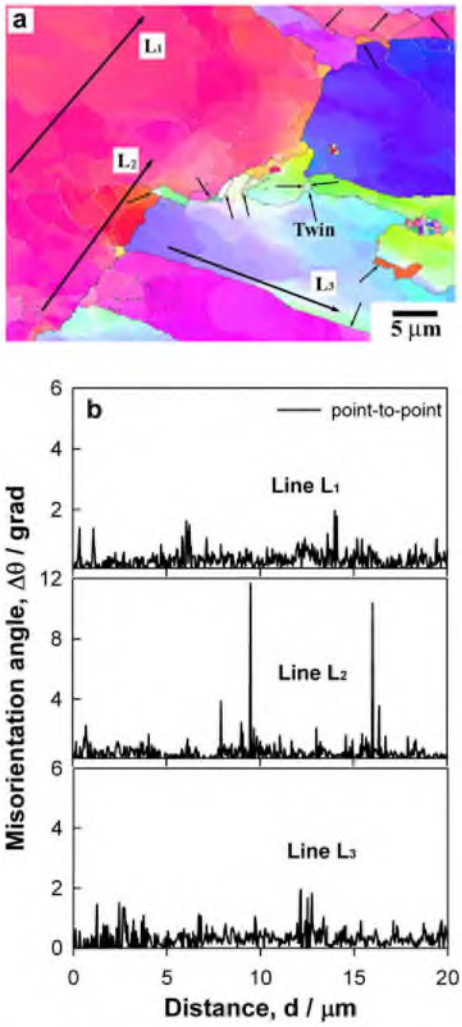


Fig. 3. Angular misorientations evolved in Ni–20%Cr alloy by compression to a strain of 0.36 at 900 °C. (a) Nucleation of DRX grains at serrated original boundaries. Twin boundaries are pointed by arrows. White and black lines correspond to subgrain/grain boundaries with misorientations of $2° \leqslant \theta < 15°$ and $15° \leqslant \theta$, respectively. (b) Point-to-point misorientation along the lines L1, L2 and L3. OIM image was obtained with a step of 40 nm.

boundary bulging is assisted by the formation of strain-induced subboundaries. Those subboundaries with medium- to high-angle misorientations can effectively separate the bulges from parent grains. The development of strain-induced subboundaries with relatively large misorientations mainly in the vicinities of initial grain boundaries is caused by the local build-up of strain gradients. The angular misorientations in grain interiors that are located far from a grain boundary do not exceed 2°, while misorientations above 10° evolve close to the initial boundary (cf. the lines L1 and L2 in Fig. 3). It should be noted that twin boundaries are not favourable sites for local misorientation development. The point-to-point misorientations along the twin boundary, i.e. the line L3 in Fig. 3, are almost the same as those that evolve in grain interiors.

In addition to the strain-induced subboundaries, the evolution of DRX grains by a discontinuous mechanism is accompanied by the formation of annealing twins. Some of the $\sum 3$ twin boundaries that evolve within the new grains are indicated by arrows in Fig. 3. In metallic materials with relatively low stacking fault energy, annealing twins were frequently observed in DRX microstructures after processing at elevated temperatures [21,29,30]. The twinning was also considered as a specific structural mechanism for discontinuous DRX [13]. The detailed investigation of deformation substructure at $\varepsilon = 0.36$ suggests that annealing twins are evolved even at the nucleation stage of DRX, as can be seen in Fig. 4. The local migration of initial boundaries leaves the twins behind. The bulge that leads to the formation of the recrystallization nucleus is enclosed by HABs. Therefore, initial grain boundaries and their junctions are preferable sites for DRX nucleation during hot working. Nucleation takes place frequently at grain boundary serrations, which are introduced by the preceding deformation, and is assisted by both the twinning and the development of strain-induced subboundaries [30,31]. The growth of new grains provides strain softening during DRX. The dislocation density behind a convex boundary is about $2 \times 10^{13}\ \mathrm{m}^{-2}$, while that at a front of the bulge is an order of magnitude higher (Fig. 4). It should be noted that the size of DRX nuclei is almost the same as the size of deformation subgrains of ~1 μm, while the average dynamic grain size is three times larger.

### 3.4. Strain-induced submicrocrystallites at 500 °C

An enlarged portion of the OIM image of Fig. 2c is represented in Fig. 5. It can clearly be seen that numerous ultrafine grains evolve at original boundaries (Fig. 5), although the shape of the $\sigma$–$\varepsilon$ curve obtained at 500 °C does not imply any recrystallization processes associated with nucleation and growth of new grains during deformation. Similar to early deformation at 900 °C, the vicinities of initial grain boundaries are characterized by a high density of strain-induced LABs. The ordinary HABs do frequently corrugate, while the twin boundaries keep their plane shape through 50% compression strain. It should be noted that some of the deformation-induced subboundaries that evolve close to corrugated grain boundaries already have high-angle misorientations. Therefore, the ultrafine grains in Fig. 5 may result from the large misorientation gradients that develop along initial boundaries.

Fig. 6a presents TEM micrographs showing the fine structure composed of largely misoriented submicrocrystallites with an average size of ~60 nm developed near the initial boundary at $\varepsilon = 0.7$. In general, this looks like the microbands that evolve upon severe deformation [27,28,32,33]. The submicrocrystallites with irregular shapes are enclosed by low- to high-angle boundaries. It can clearly be seen in Fig. 6a that these fine crystallites resulted from the development of the spatial net of deformation-induced LABs with increasing misorientations. No annealing twins were observed within such crystallites. In contrast to DRX under hot working, the new grain development is not accompanied by a decrease in the density of lattice dislocations in their interiors. The values of the dislocation density of $3 \times 10^{15}\ \mathrm{m}^{-2}$ in new fine grains and $4 \times 10^{15}\ \mathrm{m}^{-2}$ in work-hardened regions are almost the same. The development of new grains near the original boundaries, therefore, should be considered as a strain-induced phenomenon appearing during deformation at 500 °C, which does not involve thermally activated migration of grain boundaries.

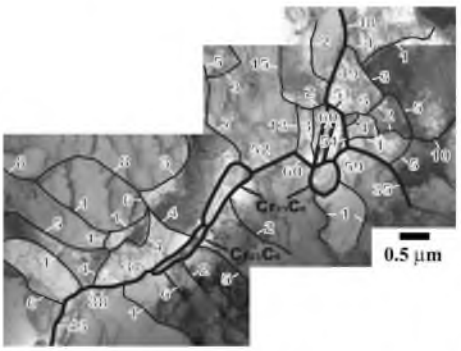


Fig. 4. Typical TEM micrograph of new (sub)grains evolved at a triple junction of original grain boundaries in Ni–20%Cr alloy deformed to $\varepsilon = 0.36$ at 900 °C.

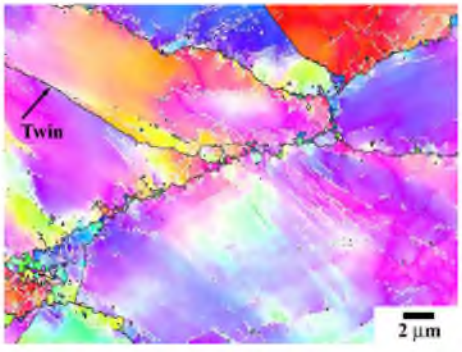


Fig. 5. OIM picture of Ni–20%Cr alloy deformed at 500 °C to $\varepsilon = 0.7$ (enlarged portion of the selected area in Fig. 2c). White and black lines correspond to subgrain/grain boundaries with misorientations of $2° \leqslant \theta < 15°$ and $15° \leqslant \theta$, respectively.

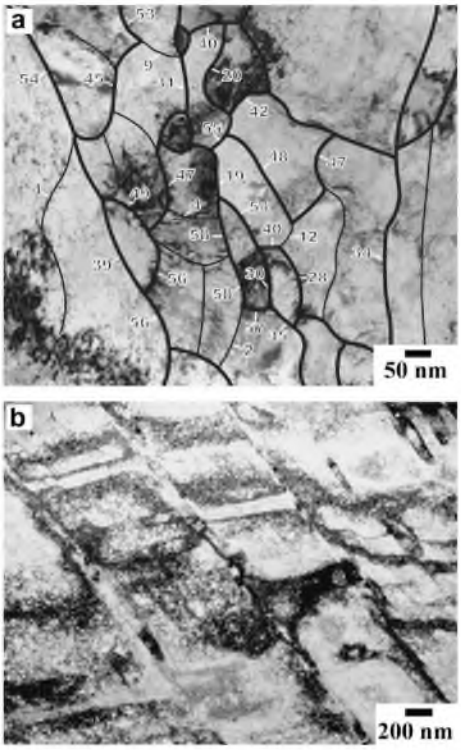


Fig. 6. Deformed (sub)structures evolved in Ni–20%Cr upon straining at 500 °C. (a) Ultrafine submicrocrystallites developed near original grain boundary at $\varepsilon = 0.7$. (b) Relatively coarse substructures within interiors of initial grains at $\varepsilon = 1.2$.

It should be noted that the size of strain-induced subgrains that evolve in the interiors of original grains at 500 °C is significantly larger than the size of highly misoriented crystallites located near initial boundaries. A typical substructure evolved inside an original grain at a strain of 1.2 is shown in Fig. 6b. The deformation substructures are represented by dense dislocation walls (DDWs) [34–36] crossing over high-density dislocations. The average distance between the DDWs is about 200 nm. Closely spaced DDWs do bound microbands, the thickness of which is well below 100 nm. It is also noted here that the DDWs of Fig. 6b may correspond to the directional LABs evolved in the grain interior in the lower side of Fig. 5. Homogeneous dislocation substructures in Fig. 6b look likely to be sheared by these DDWs. This suggests that these walls can be considered as micro-shear bands, as observed in recent studies on strain-induced grain formation in Cu [27], ferritic steel [28] and Al alloys [37].

### 3.5. DRX at 700 °C

The development of DRX grains during deformation at 700 °C is illustrated by Fig. 7. Two DRX mechanisms can operate at this temperature. It is seen that remarkable bulging takes place at the original grain boundaries, but not at the twin boundaries, after $\varepsilon = 0.36$ in Fig. 7a. An increase in strain to 0.7 leads to the development of DRX interlayers between original grains (see upper part of Fig. 7b). The

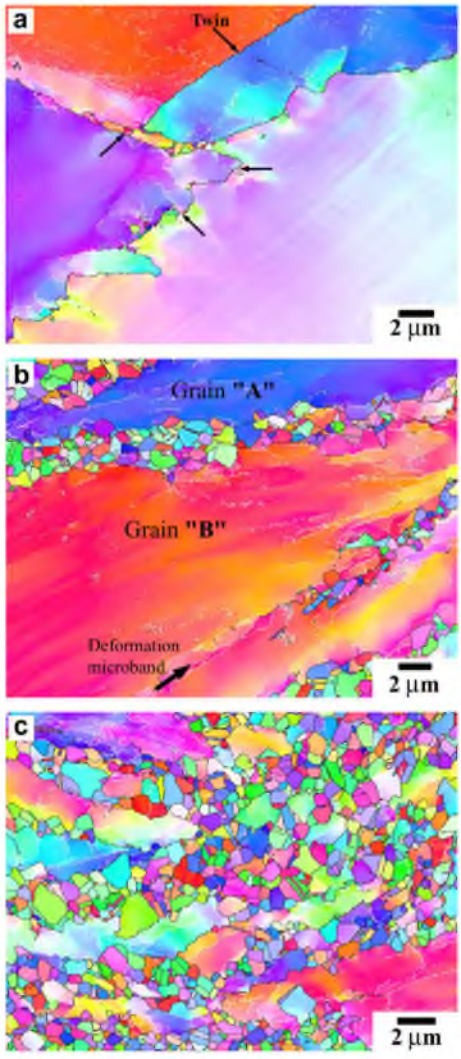


Fig. 7. Typical OIM pictures of Ni–20%Cr alloy deformed at 700 °C. (a) Bulging of serrated grain boundaries at $\varepsilon = 0.36$. Twin boundaries are pointed by the arrows. (b) DRX interlayers between original grains and along deformation microband at $\varepsilon = 0.7$. (Enlarged portion of Fig. 2b.) (c) DRX development at $\varepsilon = 1.2$. White and black lines correspond to subgrain/grain boundaries with misorientations of $2° \leqslant \theta < 15°$ and $15° \leqslant \theta$, respectively.

DRX interlayers are composed of fine recrystallized grains, many of which involve annealing twins. Upon further deformation the DRX layers expand, consuming unrecrystallized areas. This results in the almost fully recrystallized microstructure after $\varepsilon = 1.2$ (Fig. 7c). In other words, the DRX development is characterized by the propagation of the mantle of recrystallized grains towards the remains of the original grains.

On the other hand, several rather small DRX grains containing no twins appear within the initial grain interior (see the right bottom quarter of Fig. 7b). These new grains are developed at a deformation microband composed of strain-induced subboundaries. The microband thickness and, consequently, the number of strain-induced subboundaries vary along the band. The HABs enclosing the new grains evolve primarily in thick portions of a microband,

while narrow regions consist of mainly LABs. Hence, the progress of DRX in the interiors of the original grains is controlled by the density and misorientations of the strain-induced subboundaries that are involved in deformation microbands. This structural response on plastic working at elevated temperatures has been discussed in terms of CDRX [12,14,17,19].

A typical example of fine structure composed of ultrafine DRX grains that developed during deformation at $\varepsilon = 0.7$ is shown in Fig. 8. Almost all the fine grains are outlined by HABs. The deformation microstructures evolved at 700 °C are characterized by relatively high dislocation densities compared to processing at higher temperature, although the difference between DRX and work-hardened grains is not so significant. The density of dislocations within interiors of recrystallized grains is $\sim 10^{14}\,\mathrm{m}^{-2}$ and that in work-hardened portions is $6 \times 10^{14}\,\mathrm{m}^{-2}$. The presence of annealing twins indicates that the formation of new grains is assisted by the migration of grain boundaries over essentially large distances. On the other hand, the formation of DRX nuclei does not seem to be always associated with the bulging of pre-existing grain boundaries. For instance, the fine (~200 nm) dislocation-free grain marked with an asterisk at the bottom of Fig. 8, which can be considered as a DRX nucleus, is entirely delimited by HABs and should therefore grow in work-hardened surroundings. The formation of such DRX nuclei can result from the development of strain-induced subboundaries, indicating the occurrence of CDRX. The formation of a well-defined "mantle" of CDRX grains is attributed to the large orientation gradients that evolve near initial boundaries and around triple junctions because of strain incompatibilities between joint grains, leading to the evolution of strain-induced LABs [8,38]. Since such LABs are a kind of geometrically necessary subboundary [34,35], their angular misorientations increase quickly upon deformation, resulting in their transformation into HABs.

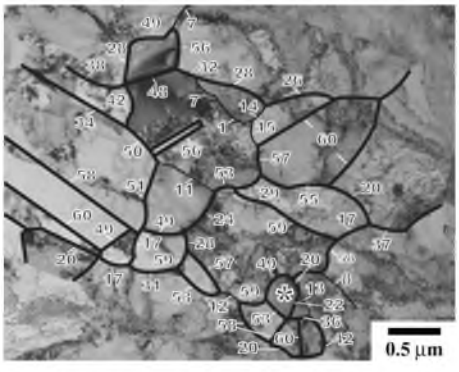


Fig. 8. DRX grains developed in Ni–20%Cr alloy strained to 0.7 at 700 °C.

## 4. Discussion

### 4.1. Variation of DRX mechanism with temperature

The present results revealed the different structural mechanisms that are responsible for the new grain development under various deformation conditions. The change in the DRX mechanisms with processing temperature is illustrated schematically in Fig. 9. Generally, new grains can dynamically develop due to the pronounced bulging of pre-existing grain boundaries followed by their long-distance migration (i.e. DDRX) or can result from a gradual increase in misorientation between deformation subgrains followed by new grain formation in situ (i.e. CDRX). The choice of DRX mechanism depends, therefore, on the critical strain, which is necessary for either the onset of grain boundary bulging or the development of highly misoriented subgrains.

Under conditions of hot deformation, the bulging is driven by stored deformation energy, i.e. high-density dislocations, and therefore requires a certain level of strain to operate [1–4,8,15,31,39]. On the other hand, remarkably larger strains are needed for the development of highly misoriented subgrains, because these are connected with the formation of strain-induced boundaries having medium to high-angle misorientations that occurs when large strain gradients evolve [5,14,15,17]. Hence, DDRX takes place at high temperatures. The rapid strain hardening associated with the increase in dislocation densities at early deformation provides a driving force for bulging under dynamic conditions followed by nucleation and growth out of DRX grains, which are almost free of interior dislocations at the beginning of the process. The growth of DRX grains at the expense of work-hardened grains takes place concurrently with work hardening, resulting in the decrease of strain-hardening rate, and then leading to strain softening when the fraction recrystallized becomes large enough. Growth of recrystallized grains removes the lattice dislocation that leads to strain softening. As a result, after

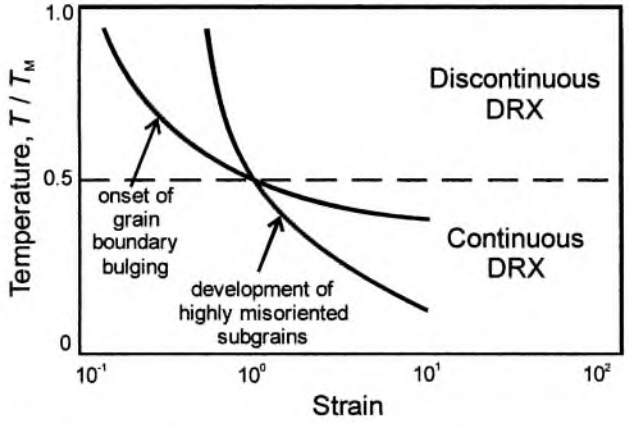


Fig. 9. Schematic drawing showing the various structural mechanisms responsible for new grain development during plastic working of Ni–20%Cr alloy.

a relatively small strain, a steady-state flow reflecting the dynamic equilibrium between strain hardening due to generation of lattice dislocations by dislocation sources and softening processes due to overlapping recrystallization cycles is attained.

Decreasing the deformation temperature slows down the grain boundary mobility. At relatively low temperatures, therefore, the onset of grain boundary bulging demands a stronger driving force, i.e. the critical strain for DDRX shifts to larger values. The temperature effect on CDRX has not been clarified in detail. Qualitatively, previous works suggest that the kinetics of new grain development by continuous reactions can be inhibited by a decrease in temperature [22,25,27,40,41]. However, the temperature effect on CDRX [40,41] seems to be weaker than that on DDRX, especially under warm to cold working conditions. Therefore, the DDRX mechanism changes to continuous one at a temperature of about $0.5T_M$. The new grains develop in areas of strain-induced subgrains, the misorientations among which are increased up to typical values for HABs. At low temperatures, the continuous reactions leading to the formation of new grains do not consume lattice dislocations due to the lack of migration of grain boundaries. CDRX leading to the development of nanometer-scale crystallites plays a similar role in the rearrangement of dislocations as the formation of low-energy dislocation structures during cold working [35,36]. It seems that CDRX provides a partial softening due to rearrangement of lattice dislocations to low-energy configurations (i.e. deformation-induced LABs). Most mobile dislocations are trapped by subgrain boundaries, leading to an increase in their misorientations and gradual transformation into HABs. At low temperatures, the value of softening associated with this process is not enough to attain the steady-state flow.

### 4.2. Relationship between DRX grain size and flow stress

Relationships between the flow stresses normalized by shear modulus and the sizes of DRX grains and deformation subgrains developed at $\varepsilon = 1.2$ are presented in Fig. 10. This figure also includes for reference the data obtained during warm deformation of copper [22], stainless steel [25] and Ni–30%Fe alloy [21]. Similar to copper and steel, the flow stresses can be related to the DRX grain size that evolves in Ni–20%Cr alloy by power-law functions with grain size exponents of about −0.7 and −0.25 in the regions of low and high stresses, respectively. The inflection point lies at the stress level of about $5 \times 10^{-3}$ to $7 \times 10^{-3}$ $G$, depending on material. This bilinear relationship reflects the change in the structural mechanisms responsible for DRX grain development under different processing conditions.

In the region of low flow stresses, i.e. under conditions of hot deformation, the development of new grains is mainly associated with the operation of the DDRX mechanism. The new grains nucleate and grow out by means of long-distance migration of pre-existing grain boundaries, leading to the strain softening on the flow curves. On the other hand,

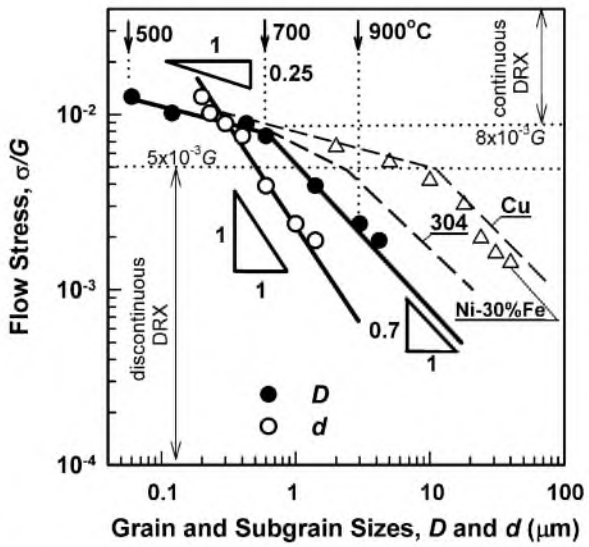


Fig. 10. Relationship between the flow stress normalized by shear modulus ($\sigma/G$) and the DRX grain size ($D$) or subgrain size ($d$) for Ni–20%Cr alloy along with the $\sigma/G$–$D$ relationships for pure copper [22,27], 304 steel [25] and Ni–30%Fe alloy [21]. The data for Ni–20%Cr were obtained under a strain of 1.2. Note that in the high flow stress region the average DRX grain sizes were measured within the small recrystallized areas located mainly near the original boundaries.

the development of new grains during plastic working in the region of high flow stresses, i.e. under conditions of warm deformation, results from the CDRX mechanism. It is interesting to note that both the continuous and discontinuous DRX mechanisms operate concurrently in the range of transition between hot and warm working (around 700 °C in the present study). This confirms that the change in DRX mechanisms occurs in a gradual manner, i.e. the contribution of different mechanisms gradually varies as the deformation conditions change. It is also worth noting that a moderate growth of CDRX grains takes place [17,40,41], which decreases the rate of strain hardening to almost zero, leading to steady-state flow.

It should be noted that the stress region of around $6 \times 10^{-3}$ $G$, where the change in DRX mechanisms occurs (Fig. 10), roughly corresponds to the breakdown of a power-law relationship between flow stress and temperature-compensated strain rate [29,42]. The flow stresses show a strong temperature and strain-rate dependence during hot deformation. In contrast, the effect of temperature and strain rate on flow stresses becomes quite weak in the region of athermal flow under warm deformation conditions. It can be concluded that the suppression of DDRX at relatively low temperatures is related to extremely slow diffusion-controlled processes that inhibit the migration of grain boundaries over large distances. On the other hand, the significant strain hardening that is associated with increasing dislocation density upon warm working creates a condition for the evolution of large strain gradients within original grains, and, consequently, results in the development of new grains in arrays of strain-induced HABs.

Since the new ultrafine grains that develop through the CDRX mechanism under warm deformation essentially originate from the strain-induced subgrains, the size of DRX grains approaches the size of these subgrains due to the hindering of HAB mobility with decreasing temperature (Fig. 10). The sizes of DRX grains and deformation-induced subgrains in Ni–20%Cr become almost the same when the flow stresses increase to $8 \times 10^{-3}$ $G$. It is interesting to note that the size of DRX grains, which develop locally at grain boundaries during warm working under flow stresses above $8 \times 10^{-3}$ $G$, is smaller than the average crystallite size among dislocation substructures within the grain interiors. It should be noted that the strain of 1.2 was not enough to complete DRX in the region of high flow stresses. The new grains were observed only in the regions with large strain gradients. In fact, the volume fractions of DRX grains were 0.02–0.07 at temperatures of 500–600 °C. The DRX grain sizes under such conditions were evaluated in the local recrystallized areas along the original boundaries. The number of strain-induced submicrocrystallites in various metals and alloys tend to increase upon severe deformation [22–28]. It can be expected, therefore, that the average size of all structural elements developed after sufficiently large strains should approach the values that are predicted by the stress dependence for CDRX.

## 5. Conclusions

The structural mechanisms during DRX of Ni–20%Cr alloy were studied in compression tests at temperatures ranging from 500 to 950 °C. The main results can be summarized as follows:

1. DDRX takes place during hot deformation under flow stresses below $7 \times 10^{-3}$ $G$. The development of DRX microstructure is associated with nucleation and growth of new grains. The latter nucleate by a bulging mechanism that is assisted by formation of both strain-induced subboundaries and annealing twins. The structural changes are characterized by the evolution of necklace-like microstructure at moderate strains followed by the propagation of DRX interlayers throughout the processed material at sufficiently large strains.
2. CDRX develops during warm working under flow stresses above $7 \times 10^{-3}$ $G$, leading to the evolution of submicrocrystalline grains not only at original grain boundaries at low strains, but also in grain interiors at medium to large strains. The new grains are evolved as a result of the formation of strain-induced boundaries with high-angle misorientations.
3. The contribution of the different DRX mechanisms to microstructure evolution progressively changes with variation of processing conditions, leading to the change in DRX mechanisms occurring in a gradual manner.
4. The relationship between the flow stress and the DRX grain size is expressed by a power-law function with grain size exponent of $-0.7$ in the range of low flow stresses (hot working conditions) or $-0.25$ in the range of high stresses (warm working conditions).


## Acknowledgements

Authors are grateful to Mr. E. Kudryavtsev, Joint Research Centre, Belgorod State University, for his assistance in specimen preparation. The financial support received from Federal Agency for Science and Innovations, Russia, under Grant No. 02.740.11.0119 is acknowledged with gratitude.


## References


[1] McQueen HJ, Jonas JJ. In: Arsenoult RJ, editor. Treatise on materials science and technology. New York: Academic Press; 1975.
[2] Sakai T, Jonas JJ. Acta Metall 1984;32:189.
[3] Derby B. Acta Metall Mater 1991;39:955.
[4] Sakai T. J Mater Process Technol 1995;53:349.
[5] Solberg JK, McQueen HJ, Ryum N, Nes E. Philos Mag A 1989;60:447.
[6] Sakai T, Ohashi M. Mater Sci Technol 1990;6:1251.
[7] Hales SJ, McNelley TR, McQueen HJ. Metall Trans A 1991;22A:1037.
[8] Humphreys FJ, Hatherly M. Recrystallization and related annealing phenomena. Oxford: Pergamon Press; 1996.
[9] Tsuzaki K, Huang X, Maki T. Acta Mater 1996;44:4491.
[10] Tsuji N, Matsubara Y, Saito Y. Scripta Mater 1997;37:477.
[11] Bhatia ML. Prog Mater Sci 1997;42:59.
[12] McNelley TR, McMahon ME. Metall Mater Trans A 1997;28:1879.
[13] Ponge D, Gottstein G. Acta Mater 1998;46:69.
[14] Gourdet S, Montheillet F. Mater Sci Eng 2000;A283:274.
[15] Sakai T, Jonas JJ. In: Buschow KH, Cahn RW, Flemings MC, Ilschner B, Kramer EJ, Mahajan S, editors. Encyclopedia of materials: science and technology, vol. 7. Oxford: Elsevier; 2001. p. 7079.
[16] Galiyev A, Kaibyshev R, Gottstein G. Acta Mater 2001;49:1199.
[17] Sitdikov O, Kaibyshev R. Mater Sci Eng 2002;328:147.
[18] Galiev A, Kaibyshev R, Sakai T. Mater Sci Forum 2003;419–422:509.
[19] Kaibyshev R, Shipilova K, Musin F, Motohashi Y. Mater Sci Eng 2005;396:341.
[20] Dehghan-Manshadi A, Barnett MR, Hodgson PD. Mater Sci Eng A 2008;485:664.
[21] Beladi H, Cizek P, Hodgson PD. Metall Mater Trans A 2009;40A:1175.
[22] Belyakov A, Sakai T, Miura H, Tsuzaki K. Philos Mag A 2001;81:2629.
[23] Humphreys FJ, Prangnell PB, Bowen JR, Gholinia A, Harris C. Phil Trans R Soc Lond 1999;357:1663.
[24] Valiev RZ, Islamgaliev RK, Alexandrov IV. Prog Mater Sci 2000;45:103.
[25] Belyakov A, Tsuzaki K, Miura H, Sakai T. Acta Mater 2003;51:847.
[26] Tsuji N. Production of bulk nanostructured metals by accumulative roll bonding (ARB) process. In: Severe plastic deformation. New York: Nova Science Publishers; 2005. p. 543.
[27] Kobayashi C, Sakai T, Belyakov A, Miura H. Philos Mag Lett 2007;87:751.
[28] Sakai T, Belyakov A, Miura H. Metall Mater Trans A 2008;39A:2206.
[29] Belyakov A, Sakai T, Miura H, Kaibyshev R. Iron Steel Inst Japan Int 1999;39:592.
[30] Wusatowska-Sarnek AM, Miura H, Sakai T. Mater Sci Eng A 2002;A323:177.
[31] Belyakov A, Miura H, Sakai T. Mater Sci Eng A 1998;A255:139.

[32] Belyakov A, Kimura Y, Tsuzaki K. Acta Mater 2006;54:2521.
[33] Belyakov A, Murayama M, Sakai Y, Tsuzaki K, Okubo M, Eto M, et al. J Electron Mater 2006;35:2000.
[34] Kuhlmann-Wilsdorf D, Hansen N. Scripta Metall Mater 1991;25:1557.
[35] Bay B, Hansen N, Hughes DA, Kuhlmann-Wilsdorf D. Acta Metall Mater 1992;40:205.
[36] Kuhlmann-Wilsdorf D. Mater Sci Eng A 1989;A113:1.
[37] Sitdikov O, Sakai T, Goloborodko A, Miura H, Kaibyshev R. Philos Mag 2005;85:1159.
[38] Belyakov A, Sakai T, Miura H. Mater Trans JIM 2000;41:476.
[39] Kaibyshev RO, Sitdikov OSh. Phys Met Metall 1994;78:97.
[40] Goloborodko A, Sitdikov O, Kaibyshev R, Miura H, Sakai T. Mater Sci Eng A 2004;381:121.
[41] Mazurina I, Sakai T, Miura H, Sitdikov O, Kaibyshev R. Mater Sci Eng A 2008;486:662.
[42] Dudova NR, Kaibyshev RO, Valitov VA. Phys Met Metallogr 2009;107:409.